Journal of Organometallic Chemistry 1019 (2024) 123312

Contents lists available at ScienceDirect

Journal of Organometallic Chemistry

journal homepage: www.elsevier.com/locate/jorganchem

Host-guest complexes of cucurbit[8]uril and [(η^5-C_5H_4R)$Mo(CO)_3CH_3$] (R = H, CO_2CH_3) for controlled release of carbon monoxide

Ana C. Gomes [a], Rodrigo P. Monteiro [a], Isabel B. Calhau [a], André D. Lopes [b], Isabel S. Gonçalves [a,*], Martyn Pillinger [a,*]

[a] CICECO – Aveiro Institute of Materials, Department of Chemistry, University of Aveiro, Campus Universitário de Santiago, Aveiro 3810-193, Portugal
[b] CCMar, and Department of Chemistry and Pharmacy, FCT, University of the Algarve, Faro 8005-039, Portugal

ARTICLE INFO

Keywords:
CO-releasing molecules
Molybdenum
Encapsulation
Cucurbituril
myoglobin assay

ABSTRACT

The monosubstituted cyclopentadienyl half-sandwich molybdenum(II) tricarbonyl complex [(η^5-$C_5H_4CO_2CH_3$)$Mo(CO)_3CH_3$] (**1**) and its 1:1 inclusion compound with cucurbit[8]uril (**1**@CB8) have been prepared and characterised by elemental and thermogravimetric analyses, powder X-ray diffraction, diffuse reflectance UV–vis, solid-state $^{13}C\{^1H\}$ MAS NMR, FT-IR, and Raman spectroscopies. The CO-releasing behaviours of **1**, **1**@CB8 and, for comparison, [(η^5-C_5H_5)$Mo(CO)_3CH_3$] (**2**) and its 1:1 inclusion complex with CB8, were assessed using a deoxymyoglobin-carbonmonoxymyglobin assay. For assays performed in the dark at 37 °C, complex **1** undergoes thermally assisted spontaneous CO release, with ca. 0.5 equivalents of CO being released after 6 h. The half-life ($t_{1/2}$) of 325 min identifies **1** as a slow releaser when compared to complex **2** bearing the unsubstituted cyclopentadienyl ligand ($t_{1/2}$ = 25 min). CO release from **1** was promoted by exposure to UV light ($t_{1/2}$ = 85 min), establishing the complex as a photochemically activated CO-releasing molecule (photoCORM). For **1**@CB8, $t_{1/2}$ for photo-assisted CO release increased to ca. 7 h, and for **2**@CB8 the dark-release $t_{1/2}$ increased to 165 min, showing that molecular acceptors like cucurbiturils can be used effectively as second-sphere ligands to modulate the CO release profile of CORMs.

1. Introduction

Carbon monoxide (CO) has been established as a signalling molecule with therapeutic properties in several illnesses including systemic and pulmonary hypertension [1,2], cardiac [3], renal [4] and small bowel [5] graft rejection, gastrointestinal diseases [6], haemorrhagic shock [7] and lung injury [8]. The clinical development of CO-based therapies has been held back to some extent by the fact that inhalational delivery of the gas is complicated by factors such as the variability in the respiratory function of patients, requirement for a hospital setting, health and safety concerns stemming from the need for large amounts of compressed CO gas in cylinders, and lack of tissue selectivity.

As an alternative method of administration, CO-releasing molecules (CORMs) were developed, aiming for a safe and controllable delivery of CO [9,10]. Over the last 20 years, a vast number of CORMs containing metals such as Fe, Mn, Co, Mo and Ru have been investigated. Molybdenum derivatives are attractive because of the essential role played by this element in the active sites of enzymes important to human metabolism [11], coupled with the expected low toxicity of molybdenum metabolites [12]. The reported Mo-based CORMs include neutral heteroleptic complexes of general formula $[Mo(CO)_m(L)_n]$ (m = 3–5), where L may be a monodentate ligand such as N-methylimidazole [13,14], glycine alkyl ester [13-15], aminopyridine derivatives [14], morpholine [16], 4-methylpiperizine [16], and isocyanoacetate derivatives [17], or a bidentate ligand such as ethylenediamine [16], 4-(2-aminoethyl)morpholine [16], 4-(2-aminoethyl)piperazine [16], and 2,2′-bipyridine derivatives [18]. Complexes with a net negative charge are known with L = halide [19–22], histidinate [22,23], and functionalized phosphines [24]. Half-sandwich organomolybdenum CORMs include [$CpMo(CO)_3X$] (Cp = η^5-C_5H_5, X = Cl) [25] and [$CpMo(CO)_3R$], where R = functionalized alkynyl ligands [25], 2-pyrone derivatives [26], and the N-maleimidato ligand [27].

The administration of CORMs as bare drugs may present pharmacological limitations owing to poor biodistribution and bioavailability (resulting from random diffusion, low cellular uptake efficiency, uncontrolled CO-release kinetics, low solubility in aqueous media), and

* Corresponding authors.
E-mail addresses: igoncalves@ua.pt (I.S. Gonçalves), mpillinger@ua.pt (M. Pillinger).

https://doi.org/10.1016/j.jorganchem.2024.123312
Received 29 May 2024; Received in revised form 6 August 2024; Accepted 11 August 2024
Available online 12 August 2024

potential toxicity associated with metal-containing decarbonylation fragments. As described in recent reviews, encapsulation of CORMs into macromolecular carriers is a promising approach to improving the properties of bare CORMs [28-30]. Mo-based CORM conjugates reported to date were obtained by the immobilization of the isocyanoacetate complexes $[Mo(CO)_3(CNCR_2CO_2H)_3]$ (R = H, Me) in metal-organic frameworks (MOFs) [31,32] and a layered double hydroxide [33], and $Mo(CO)_6$ in a MOF [34]. Encapsulation of half-sandwich CORMs such as $[CpMo(CO)_3R]$ into macromolecular carriers has not been reported in the context of CO-based therapy. Nevertheless, previous work described the encapsulation of the complexes of $[CpMo(CO)_3Cl]$ [35,36] and $[CpMo(CO)_3CH_3]$ [37] in the macrocyclic hosts β-cyclodextrin (CD), permethylated βCD (TRIMEB), and cucurbit[*n*]urils (CB*n; n* = 7, 8), and the resultant inclusion compounds were studied as supramolecular precatalysts for olefin epoxidation [36,37].

CB*n* are a relatively new family of barrel-shaped macrocycles that have great potential as drug-enhancing excipients for a range of pharmaceutical applications [38–40]. Encapsulation of drugs into CB*n* can lead to various benefits such as improved drug solubility and stability, controlled and sustained drug release, and photo-activation of prodrugs, which are all important issues in CO-based therapies with CORMs. To the best of our knowledge, there are no previous reports on modifying the CO releasing behaviour of metal carbonyl CORMs by encapsulation in CBs. In the present work, we present a new strategy for CO delivery systems based on the encapsulation of the complexes $[(\eta^5\text{-}C_5H_4R)Mo(CO)_3CH_3]$ (R = CO_2CH_3 (**1**), H (**2**)) in CB8. The CO release half-lives of the inclusion complexes, determined by a myoglobin assay, were longer than those for the corresponding bare CORMs. While the inclusion complex **1**@CB8 slowly liberated CO upon incubation in a buffer solution in the dark, irradiation with UV light resulted in a significantly accelerated release of CO, thus establishing this host-guest system as a photoactivatable CORM-carrier conjugate.

2. Experimental

2.1. Materials and methods

CHN microanalyses were collected on a Leco TruSpec CHNS 630–200–200. ICP-OES analyses for Mo were performed at the Central Analysis Laboratory, University of Aveiro, using a Horiba JobinYvon Activa M spectrometer (detection limit of ca. 20 μg dm^{-3}). Prior to analysis, solid samples (10 mg) were digested using 1 mL HF and 1 mL HNO_3 with microwave-assisted heating at 180 °C. Powder X-ray diffraction (PXRD) data were collected at rt on a Malvern Panalytical Empyrean diffractometer (Malvern Panalytical, Malvern, UK) equipped with a spinning flat sample holder and a PIXcel 1D detector set at 240 nm from the sample, in a Bragg-Brentano para-focusing optics configuration (45 kV, 40 mA). $CuK_{\alpha1,2}$ X-radiation (λ_1 = 1.540598 Å, λ_2 = 1.544426 Å) filtered with nickel foil was used. Samples were step-scanned from 3 to 70° (2θ) in 0.02° 2θ steps with a counting time of 100 s per step. Thermogravimetric analysis (TGA) was performed using a HITACHI STA 300 system at a heating rate of 5 °C min^{-1} under air. Attenuated total reflectance (ATR) FT-IR spectra were measured on a Bruker Tensor 27 spectrometer equipped with a Specac Golden Gate Mk II ATR accessory having a diamond top plate and KRS-5 focusing lenses (resolution 4 cm^{-1}, 256 scans). FT-Raman spectra were recorded in the range of 50–4000 cm^{-1} on a Bruker MULTIRAM instrument equipped with a Ni:YAG laser with an excitation wavelength of 1064 nm (resolution 4 cm^{-1}, 1000 scans). Solid-state $^{13}C\{^1H\}$ cross-polarization (CP) magic-angle spinning (MAS) NMR spectra were recorded on a Bruker Avance III 400 spectrometer (9.4 T) at 100.62 MHz with 3.7 μs ^1H 90° pulses, 3500 ms contact time, spinning rates of 10 or 12 kHz, and 5 s recycle delays. Diffuse reflectance (DR) UV–vis spectra were recorded at rt in the range of 190–900 nm using a JASCO V-780 spectrophotometer equipped with a JASCO ISV-469 integrating sphere, with Spectralon as reference material. The spectra were collected in the reflectance mode, with a bandwidth of 2 nm, a scan speed of 200 nm min^{-1}, and a data pitch of ~ 0.5. UV–vis spectra (in solution) for stability studies were collected using a Cintral 303 spectrophotometer (190–900 nm). UV–vis spectra for the Mb assays were collected using a GBC UV-vis 918 spectrophotometer. In the Mb assays with UV light (365 nm) exposure, a Velleman 15 W UV lamp was used as the light source.

The following chemicals and materials were purchased from Sigma-Aldrich (unless otherwise indicated) and used as received: (for synthesis) molybdenum hexacarbonyl, 2.4 M sodium cyclopentadienylide in THF, dimethyl carbonate, methyl iodide (99 %), anhydrous THF (≥99.9 %), diethyl ether (99.8 %) and pentane (99 %, Carlo Erba); (Mb assays) equine skeletal muscle (95–100 %, lyophilised powder), sodium dithionite, phosphate buffered saline (PBS) tablet for 10 mM solutions, carbon monoxide (99.9 %), Alphagaz Nitrogen type 1 (99.9 %, Air-Liquide), anhydrous dimethyl sulfoxide (99.9 %, Merck) and anhydrous ethanol (99.9 %, Carlo Erba). Anhydrous solvents were stored over preactivated 4 Å molecular sieves.

2.2. Synthesis

The preparation and characterisation of CB8 with the approximate composition $C_{48}H_{48}N_{32}O_{16}\cdot7H_2O\cdot3HCl\cdot1.5(CH_3COCH_3)$ were described in a previous paper [41]. To prepare the complex $[CpMo(CO)_3CH_3]$ (**2**) and its 1:1 inclusion compound with CB8 (**2**@CB8), the procedures described recently were followed [37]. Characterisation data for **2**@CB8 are provided in the Supplementary Information and are in agreement with the published data in Ref. [37].

2.2.1. $Na(C_5H_4CO_2CH_3)$

The ligand $Na(C_5H_4CO_2CH_3)$ was prepared by following a literature procedure [42]. Dimethyl carbonate (1.91 mL, 22.7 mmol) was added to a 2.4 M solution of sodium cyclopentadienylide (5.67 mL, 11.3 mmol) in THF (20 mL). The solution was refluxed for 4 h under a nitrogen atmosphere and then the solvent was removed under reduced pressure. The resultant residue was washed with diethyl ether (4 × 20 mL) and vacuum-dried for 2 h. Yield: 1.35 g, 82 %.

2.2.2. $[(\eta^5\text{-}C_5H_4CO_2CH_3)Mo(CO)_3CH_3]$ (*1*)

This procedure is based on that described by Hart et al. for the same complex [43]. $Na(C_5H_4CO_2CH_3)$ (1.35 g, 9.24 mmol) and $Mo(CO)_6$ (2.44 g, 9.24 mmol) were added to a Schlenk tube and then anhydrous THF (40 mL) was added. The mixture was refluxed for 24 h to produce a solution of the anion $[(\eta^5\text{-}C_5H_4CO_2CH_3)Mo(CO)_3]^-$. After cooling to rt, MeI (1.72 mL) was added, and the mixture was stirred at rt for 4 h. The solvent was then removed under reduced pressure. The product was extracted with pentane (2 × 20 mL) and diethyl ether (4 × 20 mL), and all the fractions were combined and concentrated, affording an orange precipitate, which was then sublimed at 80 °C and vacuum-dried for 2 h. Yield: 2.04 g, 70 %. Anal. Calcd for $C_{11}H_{10}MoO_5$ (318.13): C, 41.53; H, 3.17. Found: C, 41.72; H, 3.32. FT-IR (ATR, cm^{-1}): 3126 (w), 3116 (w), 3009 (w), 2959 (w), 2914 (w), 2845 (w), 2015 (s), 1897 (vs), 1714 (vs), 1470 (m), 1431 (m), 1414 (m), 1379 (m), 1349 (w), 1280 (vs), 1212 (w), 1191 (w), 1174 (m), 1138 (vs), 1064 (w), 1043 (m), 1028 (m), 962 (s), 930 (m), 892 (m), 837 (s), 829 (s), 785 (m), 774 (s), 585 (sh), 560 (vs), 507 (m), 483 (vs), 440 (vs). FT-Raman (cm^{-1}): 3129 (m), 3115 (m), 3008 (m), 2960 (m), 2915 (m), 2014 (m), 1943 (s), 1906 (vs), 1893 (w), 1717 (m), 1674 (w), 1472 (m), 1436 (w), 1416 (w), 1382 (w), 1285 (m), 1175 (w), 1143 (m), 1066 (m), 1045 (w), 1031 (w), 965 (w), 932 (w), 894 (m), 833 (w), 789 (w), 777 (w), 608 (w), 579 (w), 506 (w), 481 (w), 453 (s), 441 (m), 410 (m), 359 (w), 345 (m), 333 (m), 319 (w), 199 (w), 174 (m), 133 (vs), 109 (vs), 98 (vs), 62 (m). ^1H NMR (acetone-d_6, 295 K, TMS): δ = 5.92 (t, $J_{H\text{-}H}$ = 2.5 Hz, 2H, C_5H_4), 5.69 (t, $J_{H\text{-}H}$ = 2.5 Hz, 2H, C_5H_4), 3.79 (s, 3H, CH_3), 0.42 (s, 3H, CH_3) ppm. $^{13}C\{^1H\}$ NMR (acetone-d_6): δ = 239.3 (Mo-CO), 226.7 (Mo-CO), 165.2 (C=O), 98.9, 96.2, 95.8 (C_5H_4), 52.3 (CO_2CH_3), −19.6 (Mo-CH_3) ppm.

2.2.3. 1@CB8

A solution of **1** (0.08 g, 0.24 mmol) in ethanol (1.5 mL) was added to CB8 (0.40 g, 0.24 mmol), followed by Milli-Q water (40 mL), and the resultant suspension was stirred for 24 h at rt. The mixture was then centrifuged for 15 min with a velocity of 6000 rpm. The pale-cream solid was isolated by decanting the mother liquor, and vacuum-dried for 2 h at rt. Yield: 0.34 g, 79 %. Anal. Calcd for $C_{48}H_{48}N_{32}O_{16}{\cdot}C_{11}H_{10}MoO_5{\cdot}8H_2O$: C, 39.56; H, 4.16; N, 25.02; Mo, 5.35 %. Found: C, 38.90; H, 3.88; N, 26.09; Mo, 5.30 %. FT-IR (ATR, cm^{-1}): 3460 (br), 3000 (w), 2913 (w), 2024 (m), 1933 (m), 1716 (s), 1456 (s), 1428 (m), 1372 (m), 1312 (m), 1283 (m), 1221 (s), 1182 (s), 1028 (w), 966 (s), 830 (m), 800 (vs), 753 (m), 664 (m), 626 (m), 586 (m), 560 (m), 506 (m), 484 (m), 439 (m). FT-Raman (cm^{-1}): 3002 (m), 2947 (s), 2872 (m), 2747 (w), 2024 (w), 1944 (m), 1739 (m), 1427 (s), 1379 (s), 1320 (w), 1286 (w), 1228 (w), 1192 (w), 1138 (w), 1044 (w), 976 (w), 907 (m), 834 (s), 752 (m), 707 (w), 657 (w), 521 (w), 440 (s), 411 (w), 366 (m), 337 (w), 279 (w), 262 (w), 175 (m), 93 (vs). $^{13}C\ \{^1H\}$ CP MAS NMR (100.62 MHz, 12 kHz spinning rate): δ = 157.0 (C=O, CB8), 154.9 (C=O, CB8), 94.3 (C_5H_4), 72.3 (CH, CB8), 54.7 (CH_2, CB8), 52.5 (CO_2CH_3), −21.4 ($MoCH_3$) ppm.

2.3. CO-release studies

The CO-release studies were performed through the Mb assay [44] where absorption spectroscopy (in the Q-band region) is used to monitor the conversion of deoxy-myoglobin (deoxy-Mb) to carbonmonoxy-myoglobin (Mb-CO). The CO released by decarbonylation of the complexes has a high affinity for the iron centre of myoglobin, resulting in loss of the deoxy-Mb absorption band (λ_{max} = 557 nm) and appearance of two new bands (λ_{max} = 540 and 577 nm) that are characteristic of Mb-CO formation.

In a typical measurement, two stock solutions were freshly prepared in degassed 10 mM PBS buffer (pH 7.4): Mb (ca. 100 μM) and sodium dithionite (40 mg mL^{-1}). Under an inert atmosphere, the solutions were added in the following order to a sealed quartz cell (3500 μL): 1185 μL of PBS, 1500 μL of Mb, and 300 μL of sodium dithionite. Firstly, a spectrum of the resultant solution was recorded to obtain the deoxy-Mb profile (0 % Mb-CO). Due to the insolubility of the bare CORMs or inclusion complexes in aqueous buffer, 4 mM stock solutions were prepared in degassed DMSO. An aliquot of the stock solution (15 μL) was added to the sealed cell, resulting in a final complex concentration of 20 μM. The quartz cell was kept either in the dark or exposed to UV light (365 nm, E = 2.5 mW cm^{-2}), at 37 °C, with constant magnetic stirring (120 rpm). The assays were conducted over a period of 6 h, and the incubation was interrupted in intervals of 30 min to measure absorption spectra between 450 and 650 nm, with a scan speed of 200 nm min^{-1} and a slit width of 2 nm. At the end of each assay, CO gas was bubbled through the liquid phase to achieve full conversion to Mb-CO, and a spectrum was recorded to obtain the Mb-CO profile (100 % Mb-CO). The actual concentrations of Mb in solution for each assay (33–39 μM) were determined by using the known Mb-CO extinction coefficient at 540 nm (ε = 15.4 $mM^{-1}\ cm^{-1}$) [45]. The assays were carried out in triplicate. The software GraphPad Prism (version 8 for Windows, GraphPad Software, Boston, Massachusetts USA, www.graphpad.com) was used to correct the spectra at the four isosbestic points (510, 550, 570 and 585 nm), as described previously [44].

2.4. Stability studies of 1 in solution

The stability of **1** was investigated by preparing a 100 μM solution of the complex in degassed DMSO in the dark. UV–vis spectra were collected over a period of 6 h. In addition, the stability of **1** in the presence of UV light was investigated using a 100 μM degassed DMSO solution.

3. Results and discussion

3.1. Inclusion complex preparation and characterisation

The encapsulation of complex **1** in CB8 was performed by mixing, in equimolar amounts and at ambient temperature, a solution of **1** in ethanol with an aqueous suspension of the cucurbituril (Scheme 1). A cream-coloured solid was recovered after a reaction time of one day. The same procedure was used recently to prepare a 1:1 inclusion compound between the complex $[CpMo(CO)_3CH_3]$ (**2**) and CB8 (**2**@CB8) [37], which has been included in the present study to gauge the effect of the Cp substituent (CO_2CH_3) on the CO-release behaviour.

PXRD showed that the product **1**@CB8 was microcrystalline since several relatively sharp reflections were observed between 8 and 25° 2θ (Fig. 1b). The pattern is suggestive of inclusion complex formation because, firstly, it is distinct from that for as-prepared microcrystalline CB8 (Fig. 1a), evidencing a change in structure (i.e., a change in the crystal packing arrangement of CB8 molecules) caused by the encapsulation of **1**, and, secondly, it does not contain reflections indicative of pure (nonincluded) **1** (Fig. 1c).

CHN microanalyses and Mo determination by ICP-OES indicated that the initial **1**:CB8 molar ratio used in the synthesis of **1**@CB8 was retained in the final product. A 1:1 binding stoichiometry for the host-guest complex was supported by TGA (Fig. 2). The TGA curve obtained under air shows an initial weight loss step that starts just above ambient temperature and levels out at ca. 200 °C. If this step is attributed solely to the loss of water, the mass loss of 8.0 % over this temperature range agrees with the formula of $\mathbf{1}{\cdot}CB8{\cdot}8H_2O$, which is the composition suggested by the CHN and Mo analyses. The 8.0 % mass loss could have a small contribution from the thermally promoted decarbonylation of guest tricarbonyl complexes. Thus, in addition to DTG (derivative) peak maxima at ca. 75 and 100 °C (for loss of water), a weak broad peak was observed, centred at ca. 150 °C. This peak coincides with the DTG peak for complex **1** that results from the abrupt weight loss step between 80 and 170 °C (24.7 %), attributed to the decarbonylation of the complex (calcd, for 3CO, 26.4 %). It is noteworthy, however, that the TGA curve for **1**:CB8 in the range of 25–250 °C is comparable with that for CB8, and the former does not display a resolved step around 150 °C that might have been expected if the thermal behaviour of the encapsulated complex was like that for nonincluded **1**. Regarding the main decomposition step, CB8 and **1**:CB8 share the same onset temperature of ca. 290 °C, but while a single continuous mass loss is then observed for CB8 up to ca. 400 °C (DTG_{max} ~ 380 °C), **1**:CB8 displays two overlapping weight loss steps (DTG_{max} = 320, 350 (sh) °C), assigned to the simultaneous decomposition of guest **1** and CB8. As expected, complete decomposition is observed for CB8 (100 % mass loss at 540 °C). On the other hand, **1**@CB8 shows a residual mass of ca. 8.0 % across the temperature range of 400–800 °C, which agrees with the value of 8.0 % calculated on the basis that the residue is MoO_3 and the starting composition is $\mathbf{1}{\cdot}CB8{\cdot}8H_2O$.

The ATR FT-IR and FT-Raman spectra of **1**@CB8 are dominated by absorption bands that originate from the host macrocycle (Fig. 3). Since CB8 does not have bands in the range of 1800–2100 cm^{-1}, the carbonyl (C≡O) stretching modes of the guest molecule are readily observed as bands at 1933 and 2024 cm^{-1} in the IR spectrum, and 1944 and 2024 cm^{-1} in the Raman spectrum, which are blue-shifted to varying degrees relative to those for complex **1** (1897 and 2015 cm^{-1} in the IR, 1943 and 2014 cm^{-1} in the Raman). The spectral shifts, in addition to the narrowing of the IR band at 1933 cm^{-1}, are consistent with noncovalent encapsulation which places the guest molecules in a solution-like isolated environment [37]. Additionally, in the ATR FT-IR spectrum of **1**@CB8, some weak bands are present in the range of 400–600 cm^{-1} which, on the basis of previous calculations for **2** [46], can be attributed to out-of-plane MoCO deformation modes (439, 485 cm^{-1}), MoCO stretching (507 cm^{-1}), in-plane MoCO deformation (560 cm^{-1}), and MoCO bending (585 cm^{-1}). These bands are essentially unshifted

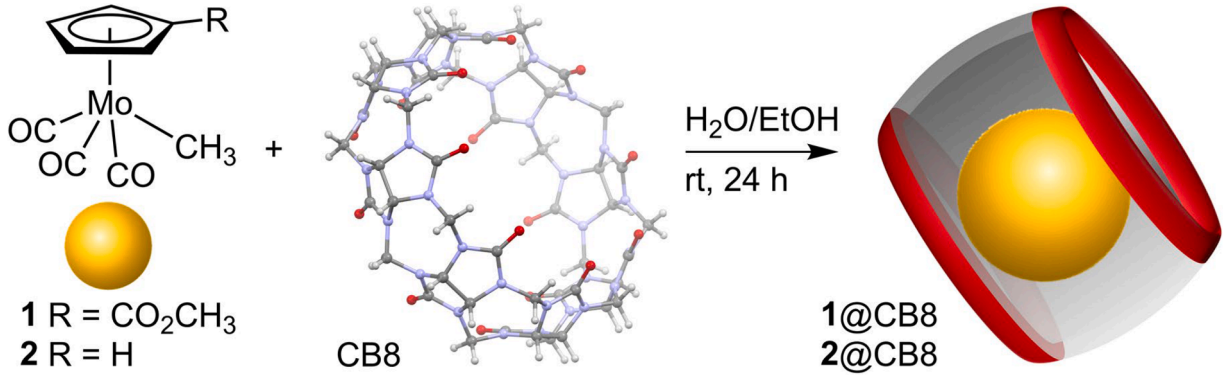

Scheme 1. Preparation of the inclusion compounds **1**@CB8 and **2**@CB8.

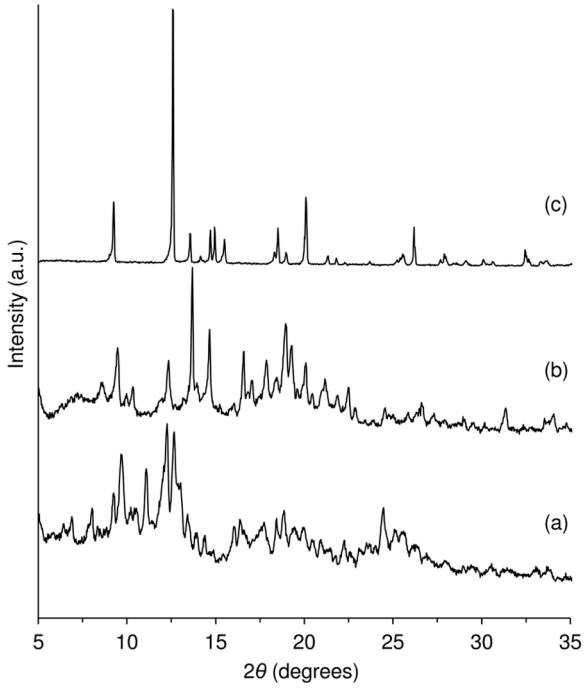

Fig. 1. PXRD patterns in the range of 5–35° 2θ of (a) CB8, (b) **1**@CB8, and (c) **1**.

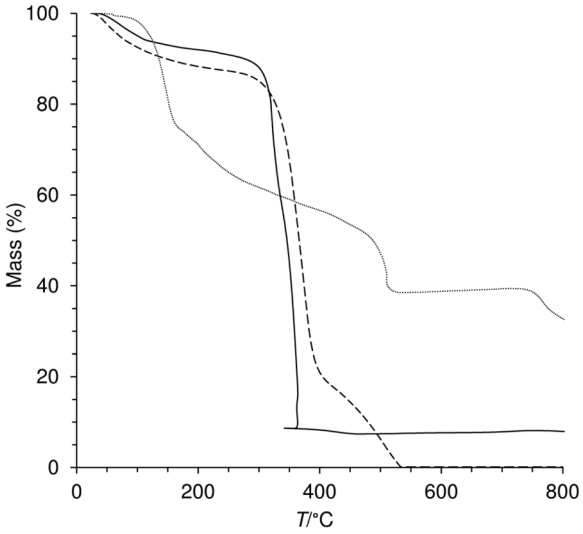

Fig. 2. TGA curves (obtained under air) of complex **1** (·····), CB8 (– – –) and **1**@CB8 (–).

relative to those for nonincluded **1**.

Fig. 4 shows the $^{13}C\{^1H\}$ CP MAS NMR spectra of pristine CB8 and **1**@CB8, and the solution spectrum of the tricarbonyl complex **1**. In accordance with the expected four-legged piano-stool geometry, the spectrum of **1** shows one resonance at 226.7 ppm for the two CO ligands *cis* to the methyl group, one weaker line at 239.3 ppm for the CO ligand *trans* to the methyl group, two adjacent resonances and one downfield-shifted signal in the range of 95.8–98.9 ppm for the cyclopentadienyl carbons, and one resonance at −19.6 ppm for the Mo-bound methyl group. Two resonances are also observed at 52.3 and 165.2 ppm for the carbon atoms of the ester group. The solid-state NMR spectrum of **1**@CB8 is dominated by the single peaks observed for the C=O, CH and CH_2 groups of the macrocyclic host, which match those observed for the pristine CB8 sample. Three guest-centred signals are observed at 94.3 (η^5-C_5H_4R), 52.5 (CO_2CH_3) and −21.4 (Mo-CH_3), with the cyclopentadienyl and Mo-CH_3 peaks showing small upfield shifts relative to those found in the solution spectrum of **1**. Resonances for the molybdenum-coordinated CO groups could not be discerned even with long acquisition times.

Fig. 5 compares the solution UV–vis spectra of **1** (EtOH, DMSO) with the DR UV–vis spectra of **1**, CB8 and **1**@CB8. In the solid-state, complex **1** exhibits a very broad absorption feature that arises from the overlap of bands with maxima in the UV and visible regions. These bands comprise a high energy component with λ_{max} ~ 285 nm, assigned to a ligand-centred n-π^* transition, a broad absorption centred around 320 nm, assigned to a metal-to-ligand charge transfer (MLCT) transition, and a more intense band that peaks at ~ 400 nm (which is responsible for the orange colour of the solid), likely stemming from overlapping MLCT and ligand field bands. These three bands are present in the solution spectra, albeit with inverted relative intensities, and it is noteworthy that the DR UV–vis spectrum of **1**@CB8 resembles more closely the solution spectra of **1** than the solid-state spectrum. These observations tie in with those made with the vibrational spectra, indicating that the half-sandwich tricarbonyl complexes are molecularly isolated by encapsulation within the CB8 cavity.

3.2. CO-release studies

To assess the stability of complex **1** in solution, degassed 100 μM solutions in DMSO were prepared and kept either in the dark or under constant exposure to UV light. UV–vis absorption spectra in the range of 200–900 nm range were collected at 30 min and then every 60 min over a period of 6 h. While no significant changes were observed for the solution kept in the dark (Fig. 6A), significant changes were observed within 30 min for the irradiated solution (Fig. 6B). The band initially present as a shoulder at λ_{max} ~ 285 nm underwent a ca. 2-fold increase

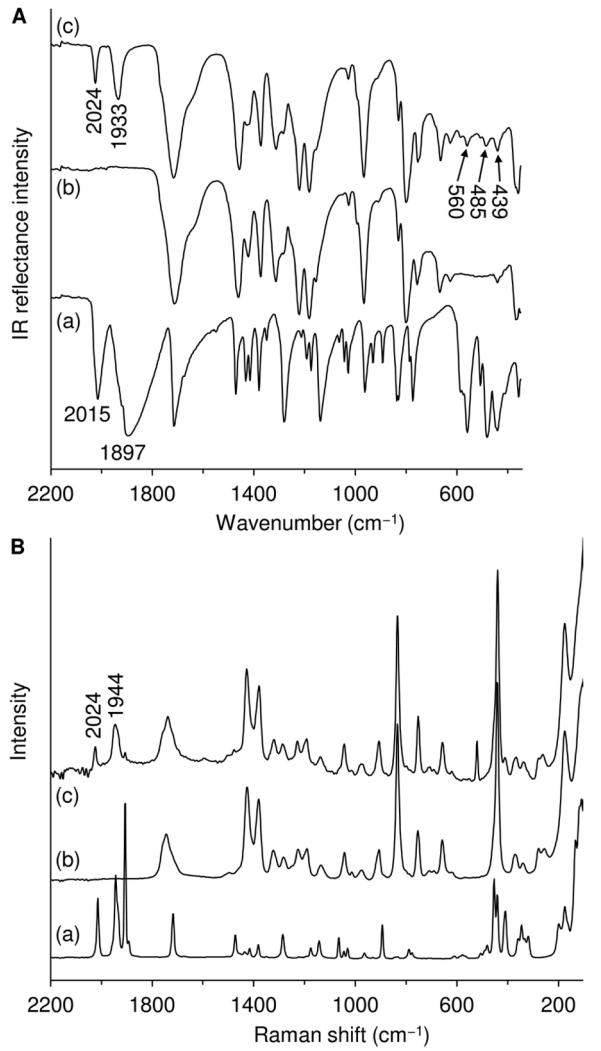

Fig. 3. ATR FT-IR (A) and Raman (B) spectra of (a) **1**, (b) CB8, and (c) **1**@CB8.

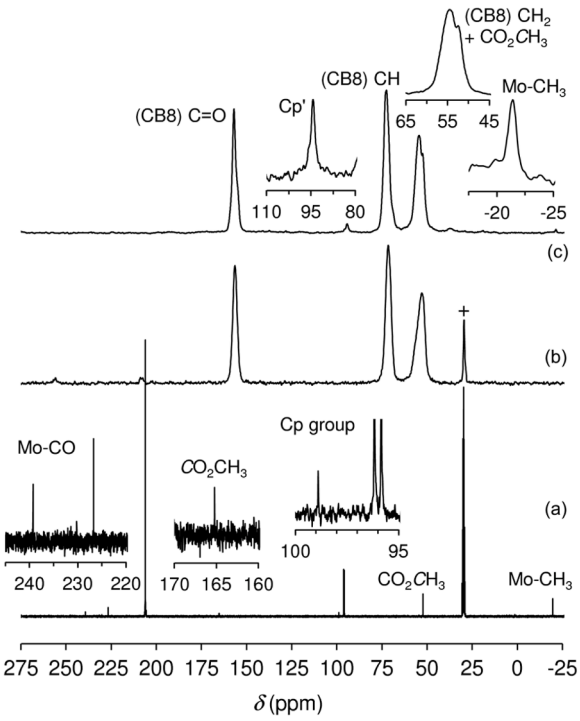

Fig. 4. $^{13}C\{^1H\}$ CP MAS NMR spectra of (b) CB8 and (c) **1**@CB8 compared with (a) the solution $^{13}C\{^1H\}$ NMR spectrum of **1** in acetone-d_6. The insets for **1** and **1**@CB8 show expansions of selected regions. For CB8 (b), the signal identified with + is due to acetone present in the as-prepared sample.

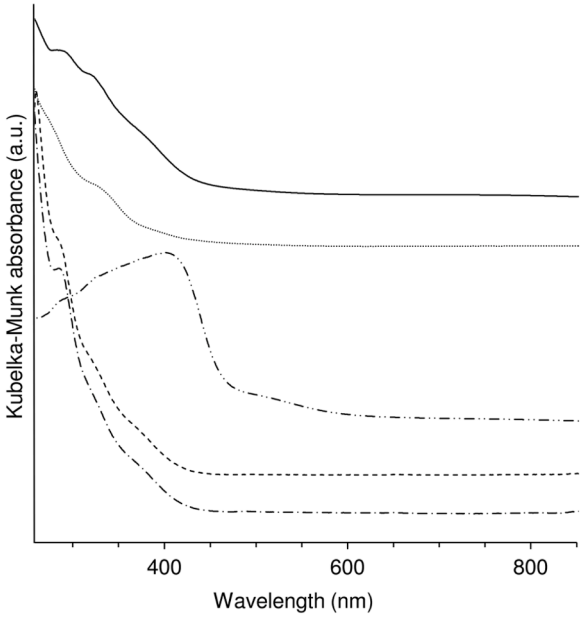

Fig. 5. Solution UV–vis spectra of **1** in ethanol (– · – · –) and DMSO (– – –), and solid-state DR UV–vis spectra of **1** (– · · – · ·), CB8 (·····) and **1**@CB8 (–).

in relative intensity and a hypsochromic shift to 274 nm. Between 1 and 6 h this band decreased in relative intensity and shifted slightly further by 4 nm to higher energy. The broad lower-energy shoulders at ca. 315 and 365 nm also underwent changes, with the former shifting slightly by a few nm to lower energy, and the latter becoming immediately less perceptible. It is generally accepted that the primary process involved in the UV photolysis of complexes like $[(CpR)Mo(CO)_3CH_3]$ (CpR = η^5-C_5H_4R) is dissociative loss of a single carbonyl ligand to give the coordinatively unsaturated 16-electron species $[(CpR)Mo(CO)_2CH_3]$ [47–53]. In the presence of a donor ligand or coordinating solvent (such as DMSO), the monosubstituted product $[(CpR)Mo(CO)_2(L)CH_3]$ may be formed, while photolysis in the absence of an external ligand may result in dealkylation, leading to the formation of CH_4 and the stable dimer $[\{(CpR)Mo(CO)_3\}_2]$. Other photodegradation products of unknown structure may be formed.

The CO-release behaviour of **1** and **1**@CB8 was evaluated by UV–vis spectroscopy using the myoglobin (Mb) assay. For comparison, the complex $[CpMo(CO)_3CH_3]$ (**2**) and its 1:1 inclusion complex with CB8 (**2**@CB8, prepared recently as a supramolecular precatalyst for olefin epoxidation [37]) were also tested. In a typical experiment, a freshly prepared solution of Mb in degassed 10 mM PBS was anaerobically reduced by an excess of sodium dithionite to yield deoxy-Mb. An aliquot of a solution of **1** in DMSO was then added (to give a final concentration of 20 μM) and the resultant solution was stirred at 37 °C in the dark. Under these conditions, complex **1** showed a slow and controlled release of CO with no plateau being reached by the end of the assay (6 h), at which point 0.54 mmol CO/mmol complex had been released (Fig. 7). Very similar results (0.55 mmol CO/mmol complex at 6 h) were obtained when ethanol was used as the solvent instead of DMSO (not shown here). In contrast, complex **2** not only released CO at a much faster rate, but also released multiple CO ligands, with a plateau of ca. 1.5 equivalents being reached at 2 h (Fig. 7, DMSO as delivery solvent).

With complex **1** being a comparatively slow releaser in the dark, the

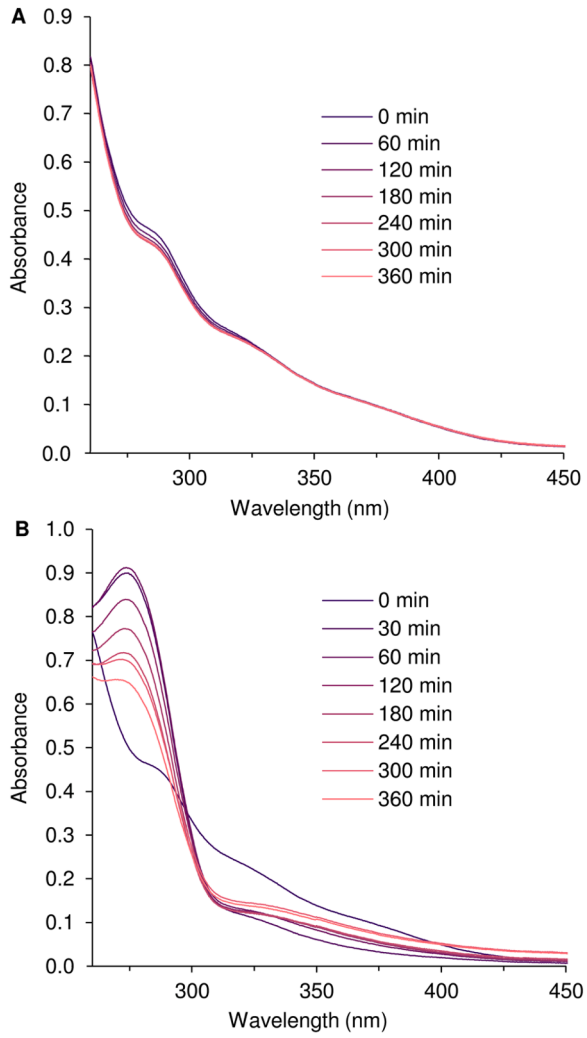

Fig. 6. UV–vis spectra (260–450 nm) of **1** in degassed DMSO (100 μM) over a period of 6 h in the dark (A) and under irradiation with UV light (365 nm) (B).

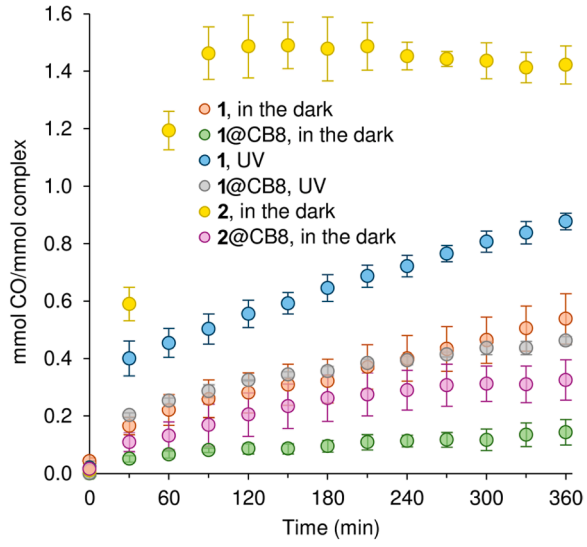

Fig. 7. Time courses of CO release for complexes **1** and **2**, and the inclusion compounds **1**@CB8 and **2**@CB8, either in the dark or under UV-light irradiation. The data values are the mean ± standard deviation of three independent assays.

potential for photochemically induced CO release was explored by performing the Mb assay with exposure to light of wavelength 365 nm from a low power UV lamp (6 W, $E = 2.5$ mW cm^{-2}). This resulted in a more rapid release of CO when compared with the thermal reaction, as shown by an increase in [Mb-CO] at 30 min from 3.3 μM (0.11 μM min^{-1}) to 8 μM (0.27 μM min^{-1}). The profile for the assays performed under exposure to UV light shows an accelerated release of CO during the first 30 min, followed by a more protracted and almost linear release for the remaining period of the assay (~ 0.03 μM min^{-1}, $R^2 = 0.996$), with no plateau being reached. After 6 h, the total CO released was 0.88 mmol CO/mmol complex. These results clearly demonstrate a significant contribution from photoinduced loss of CO. Assay durations longer than 6 h were not explored because of the limited stability of deoxy-Mb, i.e., there is an increasing risk of conversion to oxygenated Mb.

As proposed by Atkin et al. [44], the half-life ($t_{1/2}$) of CO-release, defined as the time taken for a solution of CORM with a concentration of X μM (i.e., 20 μM in the present work) to produce a solution of Mb-CO with a concentration of $X/2$ μM (i.e., 10 μM in the present work), is a convenient parameter to compare in a quantitative manner the CO-release rates of different systems. For slow releasers (e.g., systems where the release of CO does not reach 0.5 equiv. within ca. 6 h), $t_{1/4}$ can be employed instead. Table 1 compares the CO-release data for **1** and **2** with results reported in the literature for similar tricarbonyl(η^5-cyclopentadienyl)molybdenum complexes. Complex **1** stands out as a slow yet sustained releaser. Thus, for assays performed in the dark with a CORM concentration of 20 μM, the $t_{1/2}$ for **1** (325 min, entry 1) is much higher than that for **2** (25 min, entry 4) and that reported for [CpMo(CO)$_3$Cl] (14.4 min, entry 5) [25]. Even with exposure to UV light (365 nm), the $t_{1/2}$ for **1** is still relatively high (85 min, entry 2), greatly exceeding the value of 13 min recorded for the complex [CpMo(CO)$_3$(C≡C-CH$_2$O-β-D-fructopyranose)] with UV (325 nm) irradiation (entry 10) [25]. The latter photoCORM released multiple molecules of CO (ca. 2 equiv. after 1 h), while CO release from **1** approached 1 equiv. after 6 h, although as mentioned above the data indicate that the release would go beyond 1 equiv. for longer incubation times. The results with **1** emphasize how relatively small changes made to the base CORM "template" structure, in this case complexes of general formula [(CpR)Mo(CO)$_3$X], can have a dramatic influence on the CO release profile. The data in Table 1 for two η^1–2-pyrone complexes (entries 12 and 13), which differed only by the presence of a bromo substituent on the 2-pyrone ring, are an even clearer demonstration of structurally sensitive CO release behaviour [26].

According to a comparison of averaged CO and Mo-C stretching frequencies, the CO groups in **2** are more strongly bound than those in [CpMo(CO)$_3$Cl] [46]. The relatively faster CO release observed for the chloro derivative ($t_{1/2}$ ~ 14 min vs. 25 min for **2**) could therefore be due, at least partly, to having a weaker Mo-C bond. A similar analysis for **1** does not provide an explanation for why this complex is a much slower releaser than **2**, since **1** gives an average (IR + Raman) CO stretching frequency of ca. 1949 cm^{-1}, while a value of 1945 cm^{-1} was reported for **2** (vs. 1978 cm^{-1} for the chloro derivative). On this basis alone, Mo-C bond strength is unlikely to be an overriding factor controlling spontaneous CO release from complexes of the type [(CpR)Mo(CO)$_3$X] in aqueous solution. The trend in $t_{1/2}$ observed for **1** and **2**, i.e., 325 ≫ 25 min, respectively, does not parallel that reported by Motterlini and co-workers for complexes of the type [(CpR)Fe(CO)$_2$X], also evaluated by the Mb assay as spontaneous CO releasers in aqueous solution [54]. Comparing the data for the series [CpFe(CO)$_2$X] with those from [(CpCO$_2$CH$_3$)Fe(CO)$_2$X] (X = Cl, Br, I), the introduction of the CO$_2$CH$_3$ substituent resulted in faster CO release, e.g. 350 ≫ 63 min $t_{1/2}$ for X = Cl.

Fig. 7 shows the results of the Mb assays performed with **1**@CB8 either in the dark or with exposure to UV light. In both situations, encapsulation has the effect of slowing down the rate of CO release. For the assay performed with UV light irradiation, the concentration of Mb-CO after 30 min was 4 μM, which equates to a rate of 0.13 μM min^{-1}, i.e.,

Table 1
Summary of CO-release rate behaviour of **1, 1**@CB8 and related complexes.[a]

Entry	Compound[b]	[CORM] (μM)	[Mb] (μM)	Cosolv.	Dark/light	Time (min)	CO release (mol_{CO}/mol_{Mo})	$t_{1/2}$[c] (min)	Refs.
1	**1**	20	~ 38	DMSO	in the dark	360	0.54	325	This work
2		20	~ 38	DMSO	UV (365 nm)	360	0.88	85	This work
3		20	~ 38	ethanol	in the dark	360	0.55	325	This work
4	**2**	20	~ 45	DMSO	In the dark	120	1.49	25 (12)	This work
5	$[CpMo(CO)_3Cl]$	20	~ 60	–	in the dark	33.3	1.3	14.4	[25]
6	$[CpMo(CO)_3(C{\equiv}CR^1)]$	[d]	~ 60	–	–	–	0	–	[25]
7	$[CpMo(CO)_3(C{\equiv}{>}CR^2)]$	[d]	~ 60	–	–	–	0	–	[25]
8	$[CpMo(CO)_3(C{\equiv}CR^3)]$	60	~ 60	–	in the dark	120	0.037	- [e]	[25]
9		60	~ 60	–	UV (325 nm)	30	0.75	16	[25]
10		20	~ 60	–	UV (325 nm)	55	1.9	13	[25]
11						150	2.2		[25]
12	$[CpMo(CO)_3(R^4)]BF_4$	40	50	DMSO	in the dark	60	0.18	- [e]	[26]
13	$[CpMo(CO)_3(R^5)]BF_4$	40	50	DMSO	in the dark	60	1.22	13.6	[26]
14	$[CpMo(CO)_3(R^6)]$[f]	67	33.5	–	vis light	120	0.43	- [e]	[27]
15	**1**@CB8	20	~ 33	DMSO	in the dark	360	0.14	- [e]	This work
16		20	~ 36	DMSO	UV (365 nm)	360	0.46	~ 420	This work
17	**2**@CB8	20	~ 39	DMSO	in the dark	270	0.31	(165)	This work

[a] All results were obtained using the Mb assay, PBS buffer, pH 7.4, at 37 °C unless indicated otherwise.
[b] R^1 = Ph, R^2 = CH_2OCH_2Ph, R^3 = CH_2O-β-D-fructopyranose, R^4 = η^1-{O}-C{=O}-O-CMe=CH-COMe=CH (η^1–2-pyrone), R^5 = η^1-{O}-C{=O}-O-CMe=CH-COMe=CBr (η^1–2-pyrone), R^6 = η^1-*N*-imidato.
[c] $t_{1/4}$ values are given in parentheses.
[d] These complexes were insoluble in the aqueous medium used for the Mb assay, and no CO release was subsequently detected.
[e] Not determinable since CO-release did not reach 0.5 equiv. over the course of the assay.
[f] Assays performed at rt.

half of that measured for **1**. After the complete incubation time of 6 h, 0.14 equiv. of CO were released in the dark (cf. 0.54 equiv. for **1**), and 0.46 equiv. were released under exposure to UV light (cf. 0.88 equiv. for **1**). In the latter case, the half-life of CO release is estimated as ~ 7 h, which is about 5 times longer than that determined for nonincluded **1**. Nevertheless, the CO release profile for the inclusion compound indicates that the release can be sustained over a period of 6 h or more. Encapsulation of **2** in CB8 led to an even more pronounced decrease in the CO release rate in comparison to nonincluded **2** (Fig. 7), as quantified by an increase in $t_{1/4}$ for the dark release from 12 min to 165 min, and a decrease in the maximum amount of CO released (during the incubation time of 6 h) from ca. 1.5 equiv. for **2** to 0.3 equiv. for **2**@CB8 (Table 1).

4. Conclusion

A macrocyclic molecular acceptor, CB8, has been employed as part of a novel strategy to modify the CO-releasing behaviour of organomolybdenum(II) CORMs, $[(\eta^5\text{-}C_5H_4R)Mo(CO)_3CH_3]$ (**1, 2**). The spectral properties of the cyclopentadienylmolybdenum tricarbonyl derivatives in the presence of CB8 are more typical of those exhibited by the free complexes in organic solution, suggesting the formation of a true inclusion complexes. The relatively large size of the CB8 cavity, with an effective inner volume of ~ 360 $Å^3$, allows the ready formation of 1:1 complexes. The present work has shown that the CO-releasing behaviour of complexes of the type $[(CpR)Mo(CO)_3CH_3]$ can be altered dramatically by relatively subtle changes in the ligand environment, i.e., introduction of a substituent on the covalently bonded first-sphere Cp ligand, or introduction of a second-sphere macrocyclic ligand noncovalently bonded to the first-sphere ligands. Specifically, supramolecular encapsulation slows the CO delivery rate in comparison to the free CORMs, which may allow a more controlled supply of the therapeutic gas. The host-guest approach is attractive since it may have the added benefit of converting the bare CORM to a more pharmaceutically acceptable crystalline form.

CRediT authorship contribution statement

Ana C. Gomes: Writing – original draft, Visualization, Validation, Methodology, Investigation. **Rodrigo P. Monteiro:** Writing – original draft, Visualization, Validation, Methodology, Investigation. **Isabel B. Calhau:** Writing – original draft, Visualization, Validation, Methodology, Investigation. **André D. Lopes:** Validation, Resources, Methodology, Investigation. **Isabel S. Gonçalves:** Supervision, Resources, Funding acquisition, Conceptualization. **Martyn Pillinger:** Writing – review & editing, Visualization, Supervision, Resources, Funding acquisition, Conceptualization.

Declaration of competing interest

The authors declare that they have no known competing financial interests or personal relationships that could have appeared to influence the work reported in this paper.

Data availability

Data will be made available on request.

Acknowledgments

This work was developed within the scope of the project CICECO-Aveiro Institute of Materials (UIDB/50011/2020 (DOI 10.54499/UIDB/50011/2020), UIDP/50011/2020 (DOI 10.54499/UIDP/50011/2020) and LA/P/0006/2020 (DOI 10.54499/LA/P/0006/2020)), financed by national funds through the FCT (Fundação para a Ciência e a Tecnologia) / MCTES (Ministério da Ciência, Tecnologia e Ensino Superior) (PIDDAC). R.P.M. (DOI 10.54499/2020.04758.BD) and I.B.C. (DOI 10.54499/2021.05953.BD) are grateful to the FCT and the European Social Fund for a PhD grants. A.C.G. acknowledges the FCT/MCTES for an Assistant Researcher Position funded through the Individual Call to Scientific Employment Stimulus (ref. CEECIND/02128/2017; DOI 10.54499/CEECIND/02128/2017/CP1459/CT0039). The NMR spectrometers used in this work are part of the National NMR Network (PTNMR) and are partially supported by Infrastructure Project N° 022161 (co-financed by FEDER through COMPETE 2020, POCI and PORL, and FCT through PIDDAC).

Supplementary materials

Supplementary material associated with this article can be found, in the online version, at doi:10.1016/j.jorganchem.2024.123312.

References

[1] P. Failli, A. Vannacci, L.D.C. Mannelli, R. Motterlini, E. Masini, Relaxant effect of a water soluble carbon monoxide-releasing molecule (corm-3) on spontaneously hypertensive rat aortas, cardiovasc. Drugs Ther. 26 (2012) 285–292, https://doi.org/10.1007/s10557-012-6400-6.

[2] B.S. Zuckerbraun, B.Y. Chin, B. Wegiel, T.R. Billiar, E. Czsimadia, J. Rao, L. Shimoda, E. Ifedigbo, S. Kanno, L.E. Otterbein, Carbon monoxide reverses established pulmonary hypertension, J. Exp. Med. 203 (2006) 2109–2119, https://doi.org/10.1084/jem.20052267.

[3] K. Sato, J. Balla, L. Otterbein, R.N. Smith, S. Brouard, Y. Lin, E. Csizmadia, J. Sevigny, S.C. Robson, G. Vercellotti, A.M. Choi, F.H. Bach, M.P. Soares, Carbon monoxide generated by heme oxygenase-1 suppresses the rejection of mouse-to-rat cardiac transplants, J. Immunol. 166 (2001) 4185–4194, https://doi.org/10.4049/jimmunol.166.6.4185.

[4] A. Nakao, G. Faleo, H. Shimizu, K. Nakahira, J. Kohmoto, R. Sugimoto, A.M. K. Choi, K.R. McCurry, T. Takahashi, N. Murase, *Ex vivo* carbon monoxide prevents cytochrome P450 degradation and ischemia/reperfusion injury of kidney grafts, Kidney Int. 74 (2008) 1009–1016, https://doi.org/10.1038/ki.2008.342.

[5] A. Nakao, H. Toyokawa, A. Tsung, M.A. Nalesnik, D.B. Stol, J. Kohmoto, A. Ikeda, K. Tomiyama, T. Harada, T. Takahashi, R. Yang, M.P. Fink, K. Morita, A.M.K. Choi, N. Murase, *Ex vivo* application of carbon monoxide in university of wisconsin solution to prevent intestinal cold ischemia/reperfusion injury, Am. J. Transpl. 6 (2006) 2243–2255, https://doi.org/10.1111/j.1600-6143.2006.01465.x.

[6] R.A.F. Hegazi, K.N. Rao, A. Mayle, A.R. Sepulveda, L.E. Otterbein, S.E. Plevy, Carbon monoxide ameliorates chronic murine colitis through a heme oxygenase 1–dependent pathway, J. Exp. Med. 202 (2005) 1703–1713, https://doi.org/10.1084/jem.20051047.

[7] I. Nassour, B. Kautza, M. Rubin, D. Escobar, J. Luciano, P. Loughran, H. Gomez, J. Scott, D. Gallo, J. Brumfield, L.E. Otterbein, B.S. Zuckerbraun, Carbon monoxide protects against hemorrhagic shock and resuscitation–induced microcirculatory injury and tissue injury, Shock 43 (2015) 166–171, https://doi.org/10.1097/SHK.0000000000000264.

[8] Y. Joe, S.K. Kim, Y. Chen, J.W. Yang, J.H. Lee, G.J. Cho, J.W. Park, H.T. Chung, Tristetraprolin mediates anti-inflammatory effects of carbon monoxide on lipopolysaccharide-induced acute lung injury, Am. J. Pathol. 185 (2015) 2867–2874, https://doi.org/10.1016/j.ajpath.2015.07.002.

[9] K. Ling, F. Men, W.C. Wang, Y.Q. Zhou, H.W. Zhang, D.W. Ye, Carbon monoxide and its controlled release: therapeutic application, detection, and development of carbon monoxide releasing molecules (CORMs), J. Med. Chem. 61 (2018) 2611–2635, https://doi.org/10.1021/acs.jmedchem.6b01153.

[10] H.I. Choi, A. Zeb, M.S. Kim, I. Rana, N. Khan, O.S. Qureshi, C.W. Lim, J.S. Park, Z. Gao, H.J. Maeng, J.K. Kim, Controlled therapeutic delivery of CO from carbon monoxide-releasing molecules (CORMs), J. Control. Release 350 (2022) 652–667, https://doi.org/10.1016/j.jconrel.2022.08.055.

[11] R.R. Mendel, Cell biology of molybdenum, BioFactors 35 (2009) 429–434, https://doi.org/10.1002/biof.55.

[12] D.G. Barceloux, Molybdenum, J. Toxicol. Clin. Toxicol. 37 (1999) 231–237, https://doi.org/10.1081/CLT-100102422.

[13] P. Wang, H. Liu, Q. Zhao, Y. Chen, B. Liu, B. Zhang, Q. Zheng, Syntheses and evaluation of drug-like properties of CO-releasing molecules containing ruthenium and group 6 metal, Eur. J. Med. Chem. 74 (2014) 199–215, https://doi.org/10.1016/j.ejmech.2013.12.041.

[14] H. Liu, P. Wang, Q. Zhao, Y. Chen, B. Liu, B. Zhang, Q. Zheng, Syntheses, toxicity and biodistribution of CO releasing molecules containing $M(CO)_5$ (M = Mo, W and Cr), Appl. Organomet. Chem 28 (2014) 169–179, https://doi.org/10.1002/aoc.3105.

[15] W.Q. Zhang, A.C. Whitwood, I.J.S. Fairlamb, J.M. Lynam, Group 6 carbon monoxide-releasing metal complexes with biologically-compatible leaving groups, Inorg. Chem. 49 (2010) 8941–8952, https://doi.org/10.1021/ic101230j.

[16] L. Kromer, A.C. Coelho, I. Bento, A.R. Marques, C.C. Romão, The effect of specific modifications of the amine ligands on the solubility, stability, CO release to myoglobin and whole blood, cell toxicity and haemolytic index of $[Mo(CO)_4(NR_3)_2]$ complexes, J. Organomet. Chem. 760 (2014) 89–100, https://doi.org/10.1016/j.jorganchem.2013.12.009.

[17] A.R. Marques, L. Kromer, D.J. Gallo, N. Penacho, S.S. Rodrigues, J.D. Seixas, G.J. L. Bernardes, P.M. Reis, S.L. Otterbein, R.A. Ruggieri, A.S.G. Gonçalves, A.M. L. Gonçalves, M.N. de Matos, I. Bento, L.E. Otterbein, W.A. Blättler, C.C. Romão, Generation of carbon monoxide releasing molecules (CO-RMs) as drug candidates for the treatment of acute liver injury: targeting of CO-RMs to the liver, Organometallics 31 (2012) 5810–5822, https://doi.org/10.1021/om300360c.

[18] H. Pfeiffer, T. Sowik, U. Schatzschneider, Bioorthogonal oxime ligation of a $Mo(CO)_4$(N–N) CO-releasing molecule (CORM) to a TGF β-binding peptide, J. Organomet. Chem. 734 (2013) 17–24, https://doi.org/10.1016/j.jorganchem.2012.09.016.

[19] W.Q. Zhang, A.J. Atkin, R.J. Thatcher, A.C. Whitwood, I.J.S. Fairlamb, J. M. Lynam, Diversity and design of metal-based carbon monoxide-releasing molecules (CO-RMs) in aqueous systems: revealing the essential trends, Dalton Trans. (2009) 4351–4358, https://doi.org/10.1039/B822157J.

[20] A.F.N. Tavares, M. Teixeira, C.C. Romão, J.D. Seixas, L.S. Nobre, L.M. Saraiva, Reactive oxygen species mediate bactericidal killing elicited by carbon monoxide-releasing molecules, J. Biol. Chem. 286 (2011) 26708–26717, https://doi.org/10.1074/jbc.M111.255752.

[21] L.S. Nobre, H. Jeremias, C.C. Romão, L.M. Saraiva, Examining the antimicrobial activity and toxicity to animal cells of different types of co-releasing molecules, Dalton Trans. 45 (2016) 1455–1466, https://doi.org/10.1039/c5dt02238j.

[22] R.P. Monteiro, I.B. Calhau, A.C. Gomes, C. Pereira, C. Vieira, M.A.F. Faustino, A. Almeida, M. Pillinger, C.C. Romão, I.S. Gonçalves, Effect of β-cyclodextrin on the CO release kinetics and antimicrobial activity of $[NEt_4][Mo(CO)_5Br]$, J. Organomet. Chem. 1000 (2023) 122844, https://doi.org/10.1016/j.jorganchem.2023.122844.

[23] J.D. Seixas, A. Mukhopadhyay, T. Santos-Silva, L.E. Otterbein, D.J. Gallo, S. S. Rodrigues, B.H. Guerreiro, A.M.L. Gonçalves, N. Penacho, A.R. Marques, A. C. Coelho, P.M. Reis, M.J. Romão, C.C. Romão, Characterization of a versatile organometallic pro-drug (CORM) for experimental CO based therapeutics, Dalton Trans. 42 (2013) 5985–5998, https://doi.org/10.1039/c2dt32174b.

[24] E. Parera, M. Marín-García, R. Pons, F. Comelles, J. Suades, R. Barnadas-Rodríguez, Supramolecular arrangement of molybdenum carbonyl metallosurfactants with CO-Releasing properties, Organometallics 35 (2016) 484–493, https://doi.org/10.1021/acs.organomet.5b00917.

[25] W.Q. Zhang, A.J. Atkin, I.J.S. Fairlamb, A.C. Whitwood, J.M. Lynam, Synthesis and reactivity of molybdenum complexes containing functionalized alkynyl ligands: a photochemically activated CO-releasing molecule (PhotoCO-RM), Organometallics 30 (2011) 4643–4654, https://doi.org/10.1021/om200495h.

[26] I.J.S. Fairlamb, J.M. Lynam, B.E. Moulton, I.E. Taylor, A.K. Duhme-Klair, P. Sawle, R. Motterlini, η1-2-Pyrone metal carbonyl complexes As CO-releasing molecules (CO-RMs): A delicate balance between stability and CO liberation, Dalton Trans, (2007) 3603–3605, https://doi.org/10.1039/B707377A.

[27] A. Kubicka, E. Parfieniuk, E. Fornal, M. Palusiak, D. Lizińska, A. Gumieniczek, B. Rudolf, Metallocarbonyl complexes: $(\eta^5\text{-}C_5H_5)M(CO)_n(\eta^1\text{-}N\text{-imidato})$ (M = Fe, Ru, Mo, W; n = 2, 3) as new photoactive CO-releasing molecules (CORMs), J. Photochem. Photobiol. A Chem 351 (2018) 115–123, https://doi.org/10.1016/j.jphotochem.2017.10.012.

[28] H. Inaba, K. Fujita, T. Ueno, Design of biomaterials for intracellular delivery of carbon monoxide, Biomater. Sci. 3 (2015) 1423–1438, https://doi.org/10.1039/C5BM00210A.

[29] A.C. Kautz, P.C. Kunz, C. Janiak, CO-releasing molecule (CORM) conjugate systems, Dalton Trans. 45 (2016) 18045–18063, https://doi.org/10.1039/c6dt03515a.

[30] A. Carné-Sánchez, F.J. Carmona, C. Kim, S. Furukawa, Porous materials as carriers of gasotransmitters towards gas biology and therapeutic applications, Chem. Commun. 56 (2020) 9750–9766, https://doi.org/10.1039/D0CC03740K.

[31] F.J. Carmona, S. Rojas, C.C. Romão, J.A.R. Navarro, E. Barea, C.R. Maldonado, One-pot preparation of a novel CO-releasing material based on a CO-releasing molecule@metal-organic framework system, Chem. Commun. 53 (2017) 6581–6584, https://doi.org/10.1039/c7cc03605a.

[32] F.J. Carmona, C.R. Maldonado, S. Ikemura, C.C. Romão, Z. Huang, H. Xu, X. Zou, S. Kitagawa, S. Furukawa, E. Barea, ACS Appl. Mater. Interfaces 10 (2018) 31158–31167, https://doi.org/10.1021/acsami.8b11758.

[33] I.B. Calhau, A.C. Gomes, S.M. Bruno, A.C. Coelho, C.I.R. Magalhães, C.C. Romão, A. A. Valente, I.S. Gonçalves, M. Pillinger, One-pot intercalation strategy for the encapsulation of a CO-releasing organometallic molecule in a layered double hydroxide, Eur. J. Inorg. Chem. (2020) 2726–2736, https://doi.org/10.1002/ejic.202000202.

[34] A.F. Silva, I.B. Calhau, A.C. Gomes, A.A. Valente, I.S. Gonçalves, M. Pillinger, A hafnium-based metal-organic framework for the entrapment of molybdenum hexacarbonyl and the light-responsive release of the gasotransmitter carbon monoxide, Mater. Sci. Eng. C 124 (2021) 112053, https://doi.org/10.1016/j.msec.2021.112053.

[35] S.S. Braga, F.A.A. Paz, M. Pillinger, J.D. Seixas, C.C. Romão, I.S. Gonçalves, Structural studies of β-cyclodextrin and permethylated β-cyclodextrin inclusion compounds of cyclopentadienyl metal carbonyl complexes, Eur. J. Inorg. Chem. (2006) 1662–1669, https://doi.org/10.1002/ejic.200501006.

[36] S.S. Balula, A.C. Coelho, S.S. Braga, A. Hazell, A.A. Valente, M. Pillinger, J. D. Seixas, C.C. Romão, I.S. Gonçalves, Influence of cyclodextrins on catalytic olefin epoxidation with metal–carbonyl compounds. crystal structure of the TRIMEB complex with $CpFe(CO)_2Cl$, Organometallics 26 (2007) 6857–6863, https://doi.org/10.1021/om701025z.

[37] P. Neves, A.C. Gomes, R.P. Monteiro, M.J. Santos, A.A. Valente, I.S. Gonçalves, M. Pillinger, Inclusion complexes of cucurbit[*n*]Urils (n = 7, 8) with η^5-cyclopentadienyl methyl tricarbonyl molybdenum(II) and their use in epoxidation catalysis, Appl. Organomet. Chem. 38 (2024) e7412, https://doi.org/10.1002/aoc.7412.

[38] S. Walker, R. Oun, F.J. McInnes, N.J. Wheate, The potential of cucurbit[*n*]urils in drug delivery, Isr. J. Chem. 51 (2011) 616–624, https://doi.org/10.1002/ijch.201100033.

[39] A. Gu, N.J. Wheate, Macrocycles as drug-enhancing excipients in pharmaceutical formulations, J. Incl. Phenom. Macrocycl. Chem. 100 (2021) 55–69, https://doi.org/10.1007/s10847-021-01055-9.

[40] O.A.A. Alabrahim, S.A. Fahmy, H.M.E.S. Azzazy, Stimuli-responsive cucurbit[*n*]uril-based supramolecular nanocarriers for delivery of chemotherapeutics, ACS Appl. Nano Mater. 6 (2023) 3139–3158, https://doi.org/10.1021/acsanm.2c05391.

[41] A.C. Gomes, C.I.R. Magalhães, T.S.M. Oliveira, A.D. Lopes, I.S. Gonçalves, M. Pillinger, Solid-state study of the structure and host-guest chemistry of

cucurbituril-ferrocene inclusion complexes, Dalton Trans. 45 (2016) 17042–17052, https://doi.org/10.1039/c6dt02811j.
[42] W.P. Hart, D. Shihua, M.D. Rausch, The formation and reactions of (η^5-carboxycyclopentadienyl)dicarbonylcobalt, J. Organomet. Chem. 282 (1985) 111–121, https://doi.org/10.1016/0022-328X(85)87147-3.
[43] W.P. Hart, D.W. Macomber, M.D. Rausch, A new, general route to functionally substituted η^5-cyclopentadienyl metal compounds, J. Am. Chem. Soc. 102 (1980) 1196–1198, https://doi.org/10.1021/ja00523a063.
[44] A.J. Atkin, J.M. Lynam, B.E. Moulton, P. Sawle, R. Motterlini, N.M. Boyle, M. T. Pryce, I.J.S. Fairlamb, Modification of the deoxy-myoglobin/carbonmonoxy-myoglobin UV-vis assay for reliable determination of CO-release rates from organometallic carbonyl complexes, Dalton Trans. 40 (2011) 5755–5761, https://doi.org/10.1039/C0DT01809K.
[45] E. Antonini, Interrelationship between structure and function in hemoglobin and myoglobin, Physiol. Rev 45 (1965) 123–170, https://doi.org/10.1152/physrev.1965.45.1.123.
[46] S.A. Hauser, R.M. Reich, J. Mink, A. Pöthig, M. Cokoja, F.E. Kühn, Influence of structural and electronic properties of organomolybdenum(II) complexes of the type [CpMo(CO)$_3$R] and [CpMo(O$_2$)(O)R] (R = Cl, CH$_3$, CF$_3$) on the catalytic olefin epoxidation, Catal. Sci. Technol. 5 (2015) 2282–2289, https://doi.org/10.1039/C4CY01604A.
[47] K.A. Mahmoud, R. Narayanaswamy, A.J. Rest, Photochemistry of tricarbonyl (η-cyclopentadienyl)methylmolybdenum in frozen gas matrices at 12 K. infrared spectroscopic evidence for the formation of dicarbonyl(η-cyclopentadienyl) methylmolybdenum and dicarbonyl(η-cyclopentadienyl)(dinitrogen) methylmolybdenum, J. Chem. Soc. Dalton Trans (1981) 2199–2204, https://doi.org/10.1039/DT9810002199.
[48] R.B. Hitam, R.H. Hooker, K.A. Mahmoud, R. Narayanaswamy, A.J. Rest, Infrared spectroscopic evidence for carbon monoxide dissociation and radical pathways in the photochemical reactions on (η-cyclopentadienyl)(methyl)tricarbonyl-molydenum, J. Organomet. Chem. 222 (1981) C9–C13, https://doi.org/10.1016/S0022-328X(00)89028-2.
[49] R.H. Hooker, A.J. Rest, Comparative photochemistry of tricarbonyl(η^5-cyclopentadienyl)methyl- and -ethyl-molybdenum and -tungsten in poly(vinyl chloride) film matrices at 12–298 K, J. Chem. Soc. Dalton Trans. (1984) 761–770, https://doi.org/10.1039/DT9840000761.
[50] M.D. Rausch, T.E. Gismondi, H.G. Alt, J.A. Schwärzle, The Photochemically-Induced Degradation of (η^5-C$_5$H$_5$)M(CO)$_3$CH$_3$ Complexes (M = Cr, Mo, W), Z. Naturforsch. B 32 (1977) 998–1000, https://doi.org/10.1515/znb-1977-0908.
[51] E. Samuel, M.D. Rausch, T.E. Gismondi, E.A. Mintz, C. Giannotti, Photolysis of η-cyclopentadienylmethyltricarbonyl derivatives of chromium, molybdenum and tungsten: formation of paramagnetic alkyl—Metal species by photochemically-induced electron and methyl transfer, J. Organomet. Chem. 172 (1979) 309–315, https://doi.org/10.1016/S0022-328X(00)92363-5.
[52] D.R. Tyler, Photochemistry of (η^5-C$_5$H$_5$)W(CO)$_3$CH$_3$ in solution. Mechanism of (η^5-C$_5$H$_5$)$_2$W$_2$(CO)$_6$ formation, Inorg. Chem. 20 (1981) 2257–2261, https://doi.org/10.1021/ic50221a063.
[53] D.L. Mohler, J.R. Downs, A.L. Hurley-Predecki, J.R. Sallman, P.M. Gannett, X. Shi, DNA cleavage by the photolysis of cyclopentadienyl metal complexes: mechanistic studies and sequence selectivity of strand scission by CpW(CO)$_3$CH$_3$, J. Org. Chem. 70 (2005) 9093–9102, https://doi.org/10.1021/jo050338h.
[54] D. Scapens, H. Adams, T.R. Johnson, B.E. Mann, P. Sawle, R. Aqil, T. Perrior, R. Motterlini, [(η-C$_5$H$_4$R)Fe(CO)$_2$X], X = Cl, Br, I, NO$_3$, CO$_2$Me and [(η-C$_5$H$_4$R)Fe(CO)$_3$]$^+$, R = (CH$_2$)$_n$CO$_2$Me (n = 0–2), and CO$_2$CH$_2$CH$_2$OH: a new group of CO-releasing Molecules, Dalton Trans. (2007) 4962–4973, https://doi.org/10.1039/B704832G.